Available online at www.sciencedirect.com
SCIENCE DIRECT®
International Journal of Heat and Fluid Flow 25 (2004) 209–222
International Journal of HEAT AND FLUID FLOW
www.elsevier.com/locate/ijhff

Optical studies of boiling heat transfer: insights and limitations

David B.R. Kenning *

Department of Engineering Science, Oxford University, Parks Road, Oxford OX1 3PJ, UK

Abstract

Optical studies provide valuable insights into the complex mechanisms of boiling heat transfer but the large gradients of temperature (and therefore of refractive index) deflect light and multiple reflections at interfaces limit the distance over which observations can be made. Optical measurements are thought of as non-intrusive but this is rarely true. Because they are difficult and time consuming, they constrain the design of boiling experiments and are applied to limited ranges of conditions. There is a risk that deductions from the observations will be applied (not necessarily by the authors) more generally than is justified. These characteristics of optical studies are illustrated by examples from forced convective film boiling on spheres and pool nucleate boiling.

Keywords: Film boiling; Nucleate boiling; Optical studies

1. Optical studies of boiling

Most boiling systems are asymmetrically three dimensional and extensive, with highly transient and possibly chaotic dynamics. Much of our understanding of their beautifully complicated behaviour has come from high-speed optical observation of the motion of liquid–vapour interfaces, originally by cine camera and more recently by video camera. The advantages of video recording, e.g. on-line adjustment of focus and lighting, rapid review, economy and convenience of format for computer analysis of the data, come at the price of a significant reduction in resolution compared to recording on film. Resolution matters because the interacting phenomena in boiling cover length scales varying by many orders of magnitude. In addition to direct observation, the optical techniques deployed in single phase heat transfer have been applied to boiling, e.g. holographic interferometry, PIV, liquid crystal and infra-red thermography, as well as optical methods of sizing small bubbles and drops. All optical methods have the potential advantage of recording data simultaneously at many points in two- or three-dimensional fields.

The characteristics of boiling that make optical methods attractive also cause difficulties in their application. Boiling is accompanied by high-heat fluxes at boundaries, causing large gradients of refractive index in the liquid that deflect light rays, which are also absorbed by the liquid and refracted and reflected at the many liquid–vapour interfaces. In single phase forced convection, heat fluxes may be adjusted to match the optimum sensitivity of a particular optical method. The non-linear nature of boiling precludes this option. The large optical disturbances may mean that the shapes of interfaces are distorted, or that certain regions are not observable from particular angles, as in the mirage effect at the bases of bubbles growing on a heated wall, discussed by Cooper (1983) in relation to a long series of experiments on the triggered growth of single bubbles observed from the side (e.g. Cooper and Chandratilleke, 1981). Cooper demonstrated the potential errors in the interpretation of the contact between the base of a bubble and a wall by suspending a 4 mm steel ball 0.4 mm above a wall that was subjected to a step increase in temperature, creating a refractive index boundary layer that gradually increased in thickness and decreased in gradient (Fig. 1). In the early stages, the boundary layer acted like a mirror situated slightly above the wall, reflecting the underside of the bubble. Later, as the boundary layer grew and was distorted by the onset of convection, the sphere was apparently attached to the wall by a stalk that eventually ruptured as the ball "detached". Mayinger (1995), in his much more detailed review of advanced optical methods at a previous Conference in this series, showed that holographic

* Tel.: +44-1865-273-000; fax: +44-1865-273-010.
E-mail address: david.kenning@eng.ox.ac.uk (D.B.R. Kenning).

0142-727X/$ - see front matter © 2003 Elsevier Inc. All rights reserved.
doi:10.1016/j.ijheatfluidflow.2003.11.010

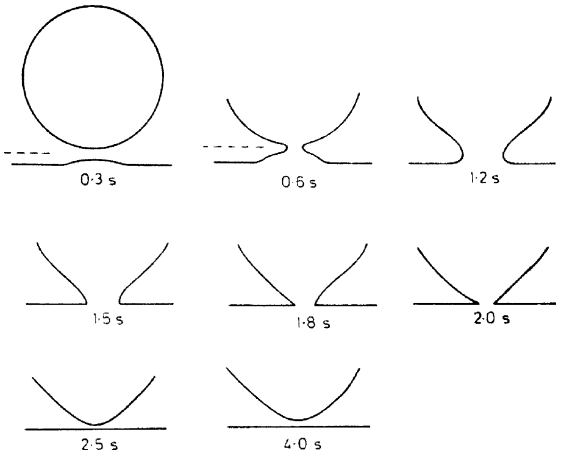

Fig. 1. Mirage demonstration (Cooper, 1983).

interferometry could measure the temperature gradients at the boundaries of bubbles away from the wall but could not resolve gradients at the base of a bubble or very close to the wall itself. The amount of deflection depends on how much of the optical path to the camera lies within the region of high temperature gradient, which is maximised for a plane wall and requires careful assessment for bubbles viewed in profile on the boundary of a cylinder or sphere. This well-known difficulty is rarely discussed in papers on the apparent contact angle of growing bubbles.

The mirage is an example of direct misinformation by optical distortion. The potential for distortion of the understanding of boiling is present in less obvious forms when the limitations of particular optical techniques require experiments to be performed under special conditions that are not typical of boiling applications.

Optical access may be limited to edge regions that are atypical of the interior or the system may have to be so simplified that some significant effects are excluded, e.g. studying bubble growth at a single nucleation site in the absence of disturbances from other bubbles. Viewing through a transparent heated wall, to overcome the difficulties of viewing bubbles on the wall from the fluid side, may involve wall bulk properties and surface conditions that differ widely from boiling on the wall of a heat exchanger.

Some optical techniques have limited ranges of application, e.g. wall temperature measurement by liquid crystals is limited to boiling on thin walls, which influences the boiling processes; the low frequency response excludes the study of boiling at large subcooling or high reduced pressure (Kenning, 2001).

Visual recordings of very high-speed events may be of limited duration and therefore not a representative sample. When an optical technique is applied over a long period of observation, it produces embarrassingly large quantities of data, requiring computerised analysis. Manual interpretation is slow and has to be confined to a few events: there is a natural inclination to choose the "best" examples of a phenomenon, e.g. those of largest scale, without determining their statistical significance. A practical difficulty of presentation is that the human brain can often pick out events from moving images that are difficult to demonstrate convincingly in a sequence of printed still pictures.

All boiling experiments with optical measurements are difficult to perform. Time and funding may run out before a technique has been fully developed or exploited, limiting the range of data obtained.

The greatest risk of distortion lies in the inappropriate application of data beyond their proven range of validity. This is an exciting time, in which the combination of old and new experimental techniques with computerised analysis offers new insights into the complex phenomena of boiling, which can then be incorporated in numerical simulations of increasing sophistication. Nevertheless, each technique has its limitations. Readers of papers must be aware of these and guard against applying findings to conditions for which they may not be valid.

In the remainder of the paper, some of the features of optical studies noted above are illustrated by work performed at Harwell and Oxford on forced convective film boiling on spheres and more generally on pool nucleate boiling on horizontal plates.

2. Forced convective boiling on spheres

2.1. Modelling approaches to fuel-coolant interactions

During a severe accident to a water-cooled nuclear reactor, molten core material at around 3000 °C might fall into pressurised, subcooled water, causing a fuel-coolant interaction with explosive evaporation during a period of self-excited intimate mixing. The energy release would depend on a preceding period of coarse mixing, with relatively slow cooling of the falling molten drops by stable film boiling. As a contribution to estimating the heat transfer during coarse mixing, a series of experiments were performed at Harwell and Oxford on film boiling on spheres at temperatures much lower than 3000 °C. The experiments all employed transient measurements of the temperature of preheated spheres brought into sudden motion relative to water at atmospheric pressure:

(a) Single nickel-plated copper spheres 10 and 20 mm in diameter supported on a thin-walled tube, driven downwards into water for a distance of 200 mm (Aziz, 1986; Aziz et al., 1986). The sphere temperature was measured by a single embedded thermocouple with its junction 0.2 mm from the front stagnation point. The maximum initial sphere tem-

perature was 513 °C. The water temperatures ranged from 50 to 100 °C. Some experiments were performed with steam bubbles injected at the bottom of the pool of saturated water to create a bubbly mixture of 2.5% void fraction. The sphere velocity ranged from 0 (after initial immersion) to 1.8 m/s.

(b) Single nickel-plated copper spheres, diameters 16–32 mm, in free fall trailing a thermocouple lead in water for a distance of 1.2 m at terminal velocities of 1.8–2.2 m/s, maximum initial sphere temperature 700 °C (Zvirin et al., 1990).

(c) Single molten brass drop, diameter 8 mm, heated and levitated electromagnetically, held stationary round a sheathed thermocouple and immersed in upward turbulent flow of water at 0.1–0.6 m/s in a 16 mm bore silica tube. Initial drop temperature 1200 °C, solidification temperature ~915 °C (Correll, 1989; Correll and Kenning, 1992).

(d) Solid spheres, diameter 8 mm, in stationary arrays in a 50 mm × 50 mm duct at solid volume fractions 0.11, 0.19, 0.46, preheated to 630 °C then exposed to flows of saturated water and water–steam mixtures (Chen and Kenning, 1996).

2.2. Single solid spheres

Experiments on solid spheres have the considerable advantage that there is no risk of an accidental explosion but they have to be performed at temperatures far below those relevant to reactor accidents. They can only indicate possible physical mechanisms. However, the data are relevant to other industrial processes such as continuous casting and metallurgical heat treatment, apart from differences in geometry.

The vapour flows around the solid spheres in (a) were recorded with the spheres back-lit by a short-duration flash unit. Distortion of the image by the cylindrical vessel was avoided by cementing on a water-filled chamber with a plane glass front. Cine films recorded at 500 Hz did not have sufficient resolution to record events ranging in scale from single bubbles less than 0.1 mm diameter to vapour wakes more than 50 mm long so most of the recordings were single shot still photographs. These provide the researcher with high resolution but there is a practical difficulty in passing this on to the readers of publications because of constraints on space and the quality of half-tone printing. This paper

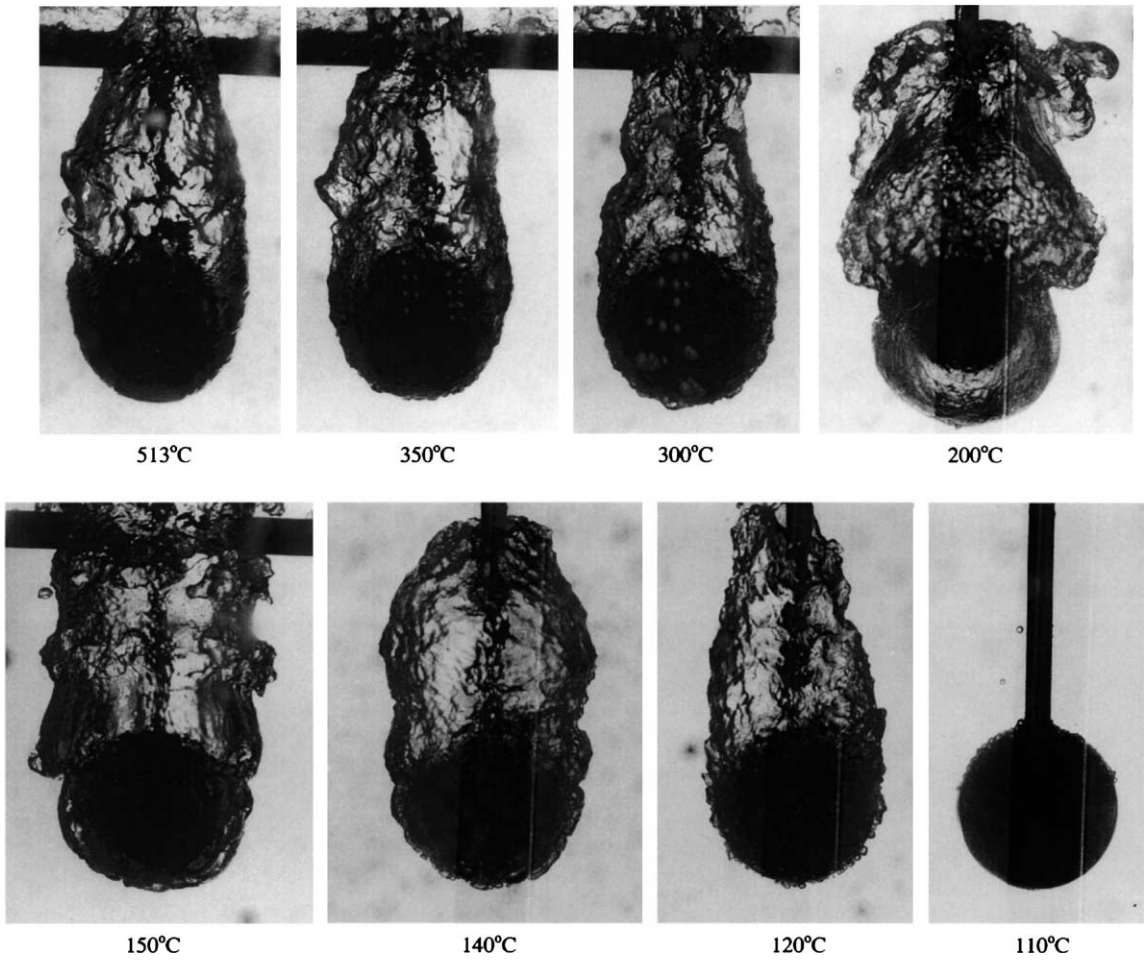

Fig. 2. Boiling on 20 mm sphere in water at 100 °C, velocity 0.9 m/s.

includes some photographs taken by Aziz (1986) that have not been published before.

Fig. 2 illustrates the effect of sphere temperature at a fixed velocity of 0.9 m/s in saturated water. (Each picture is for a separate run at a different initial temperature.) At 513 °C, the front of the sphere is covered by a thin wavy film and there is a large closed vapour cavity at the rear. This pattern persists down to 350 °C, at which point bubble-like disturbances develop on what still appears to be a continuous film on the front of the bubble, their size range widening to 0.1–3 mm with further reduction to 300 °C. At 200 °C, there is a sudden development of a pulsating instability observed by previous workers (e.g. Stevens and Witte, 1971), in which a shell of vapour round the sphere grows and collapses radially, despite the high stream velocity, releasing vapour periodically into the wake. The wake then looks like the hovering bubbles above small-diameter horizontal discs in high-flux nucleate boiling, as described by Katto (1992). At 150 °C, there is still a pulsating discharge of vapour but there appear to be breaks in the vapour film near the front stagnation point during the collapse phase. At 140 °C, the pulsations cease so the wake cavity becomes steady again; there is nucleate boiling on the front of the sphere, with large patches of vapour ahead of the wake. At 120 °C, nucleate boiling is fully established on the front half of the sphere, still with a large wake cavity. The bubbles appear to have large contact angles but this may be affected by the mirage effect. At 110 °C, a large part of the bubble is clear of bubbles but it is difficult to identify its exact boundary. There is a small patch of tiny bubbles at the front stagnation point and a patch of larger bubbles at the rear in place of the wake cavity, but no evidence of activity.

At the same velocity of 0.9 m/s but with the water subcooled by 10 K (Fig. 3), there is a striking change in the appearance of the vapour film and wake at sphere temperatures above 455 °C because the short-wavelength disturbances are suppressed. There is a sudden change in the profile of the film just before the midpoint of the sphere, apparently coinciding with separation of the external flow. At temperatures approaching 395 °C, the film everywhere develops an entirely different small-

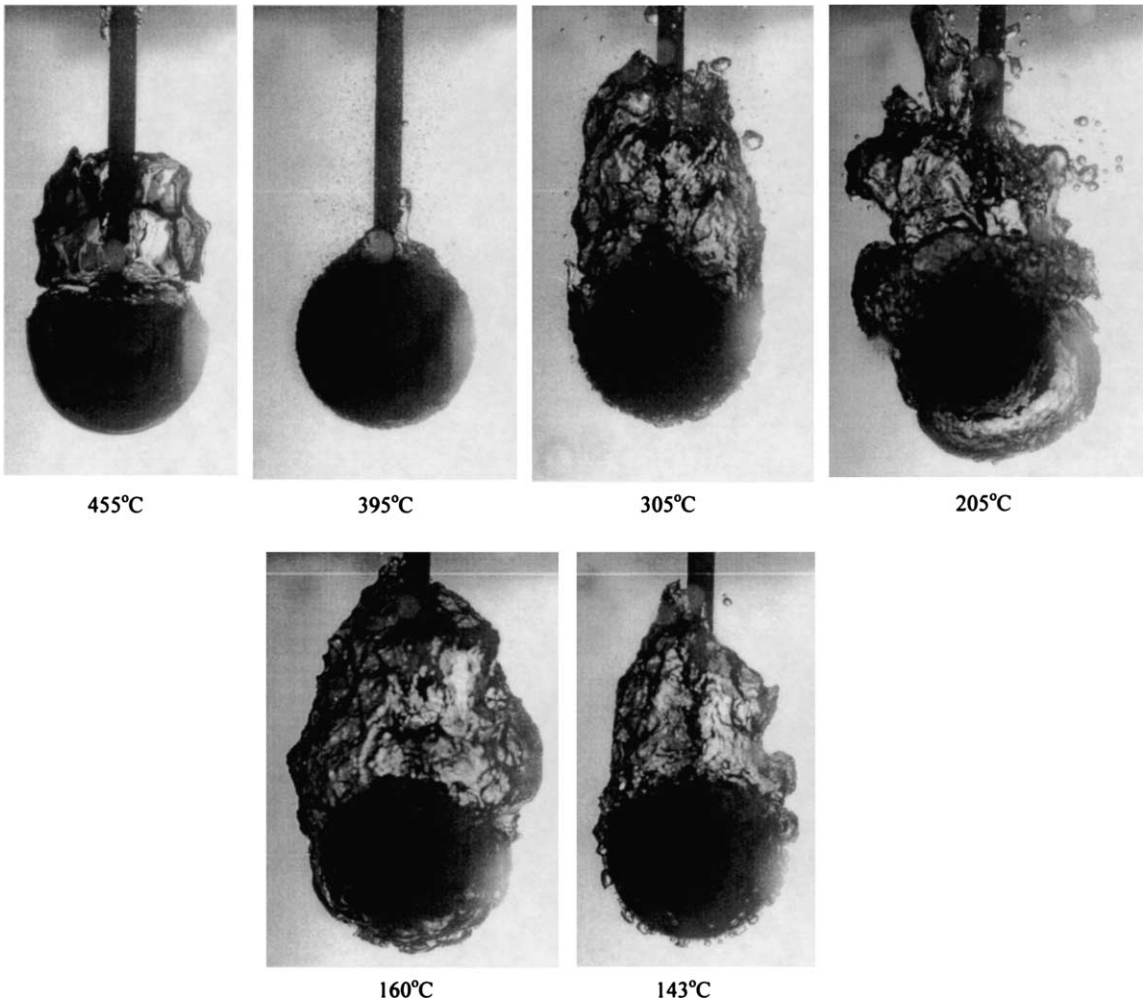

Fig. 3. 20 mm sphere in water at 90 °C, velocity 0.9 m/s, decreasing temperature.

scale instability, entering the noisy micro-bubble regime. Tiny bubbles are thrown off the surface and are swept along by the external flow. It appears that the intense mixing driven by the bubbles is sufficient to postpone flow separation and to allow the heat from the sphere to be carried away by the liquid boundary layer, because the vapour wake is almost completely suppressed. At 305 °C, micro-bubble boiling is replaced by larger scale disturbances on a thicker film and the wake cavity reappears. Disturbed film boiling ends in the pulsating instability at 205 °C, although the disturbances are less symmetrical than in saturated liquid. At temperatures below 160 °C, nucleate boiling is established on the front part of the sphere and the wake becomes steady again.

Micro-bubble boiling becomes more violent as the subcooling is increased (Fig. 4). At 50 K subcooling, the irregular jets of micro-bubbles penetrate far into the bulk flow, despite its velocity of 0.9 m/s. The onset of micro-bubble boiling is sensitive to the combination of subcooling and velocity (Fig. 5). At 513 °C and 20 K subcooling, the vapour pattern at 1.4 m/s is not greatly different from the pattern in saturated water at 0.9 m/s (Fig. 3). The front of the sphere is covered by a thin film with small-scale disturbances and only a few indications

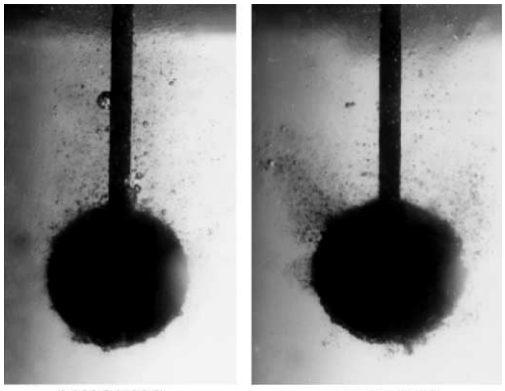

Fig. 4. Micro-bubble boiling on 20 mm sphere, velocity 0.9 m/s, increased subcooling.

of local micro-bubble production; there is a vapour-filled wake cavity. At 1.3 m/s, the wake cavity has disappeared, micro-bubble boiling is established on the rear half of the sphere and there is some slight activity on the front half. At 0.56 m/s, the film on the front of the sphere is free of disturbances, except for a train of very regular waves ahead of the midpoint, and micro-bubble boiling is established on the rear half of the sphere. At 0.51 m/s, the regular waves have moved further towards the midpoint of the sphere, which is otherwise entirely encased in a thin, smooth film. The combination of refraction and reflection in the vicinity of the waves gives an exaggerated impression of their amplitude. It is not possible to measure the thickness of the smooth vapour film accurately from these photographs. The photographs illustrate the delicate balances between the influences of wall superheat, bulk subcooling and external velocity field that determine the shape and stability of the vapour film and consequently the rate of heat transfer.

Observations in the free fall experiments (b) at higher sphere temperatures and velocities of about 2 m/s confirmed the general pattern of behaviour in (a) and showed that the onset of micro-bubble boiling could occur at a sphere temperature of 670 °C in water subcooled by 38 K. The onset was accompanied by lateral forces sufficient to divert falling spheres from their vertical path.

2.3. Single molten drops

The measurement of cooling curves for a molten drop from temperatures of 1200 °C in experiments (c) presented severe problems of electrical interference between systems, synchronisation of the short-running time of the high-speed camera with the quench and of optical access through the levitation coils (Fig. 6). Light emission by the drop, decreasing during the quench, made it difficult to achieve satisfactory lighting. Simultaneous cine films and recordings of temperature above the melting point were only achieved in runs at high

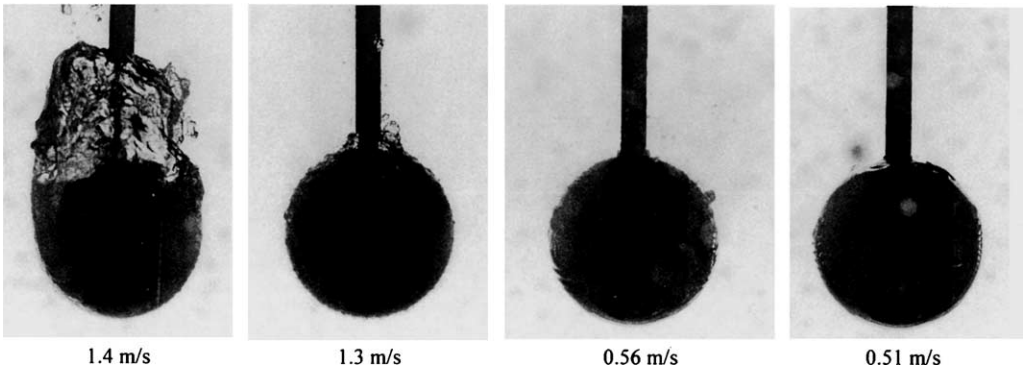

Fig. 5. 20 mm sphere at 513 °C in water at 80 °C.

Fig. 6. Electromagnetically heated/levitated drop.

Fig. 8. Solidified drop.

subcoolings of 36–48 K and low velocities of 0.1–0.3 m/s. The sphere was levitated and melted initially in a nitrogen atmosphere, with the water flow diverted through a bypass. Once the sphere reached the required temperature, the water was redirected so that its free surface rose to cover the drop. In the very early stages as the water covers the lower half of the drop, it is possible to see in the cine recordings a reasonably smooth vapour film. As the water rises above the drop, the flow becomes violently disturbed. Still frames are uninformative (Fig. 7), but by repeated viewing of the cine films combined with clues from the examination of the solidified drop, it is possible to identify events associated with interactions between the subcooled coolant and the molten drop.

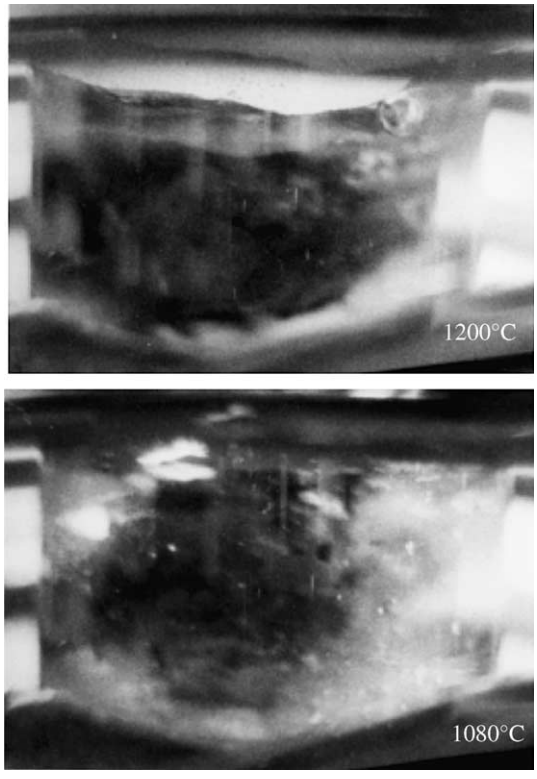

Fig. 7. Molten drop, 0.1 m/s, 48 K subcooling.

The surface of the solidified drop is covered with small pits indicative of bombardment by small water droplets and there is evidence of a few much stronger events in which water has penetrated deeper, expelling material from a crater or as a jet or a balloon-like shell (Fig. 8). The expelled material is cooled more rapidly to solidification than the drop. In one filmed example, a protuberance maintains its identity for a short time while it is gradually reabsorbed by the molten drop. In the one experiment at a higher velocity of 1.0 m/s, 55 K subcooling, the drop at 1150 °C disintegrated on contact with the water. Highly subcooled convective film boiling on a molten drop is an example of a process which, as a consequence of its disturbed nature, is almost impossible to observe optically in close detail. Film boiling at low subcooling after solidification, even on a deformed drop, is more orderly and closer to the experiments on solid spheres (Fig. 9). It may be that experiments on molten drops at low subcooling would have been more observable but financial support for the project was exhausted before they could be achieved.

2.4. Arrays of solid spheres

In a swarm of drops or spheres, each drop falls through a non-equilibrium liquid–vapour mixture cre-

Fig. 9. Solidified drop, 0.3 m/s, 10 K subcooling.

ated by the other particles. These conditions were simulated in the experiments (d) with arrays of 8 mm stainless steel spheres held in a duct on thin wires in 10, 11 or 24 layers at spacings of 10, 8.3 and 6.2 mm respectively, corresponding to sphere volume fractions of 0.11, 0.19 and 0.46. Two spheres in the penultimate layer were made of bronze, soldered to 0.8 mm diameter sheathed thermocouples. The arrays were preheated to about 650 °C by a flow of hot air. Saturated water was then pushed up through the duct from a reservoir incorporating a large piston (Fig. 10) at a superficial velocity of about 1.5 m/s. Saturated steam from a separate vessel could be mixed with the water ahead of the test section but initiation of the steam flow before the water caused precooling of the array to about 350 °C. Additional steam was generated at a variable rate by quenching of the array, so steady flow conditions were not established at the exit. The quenching technique for measuring heat transfer rates, which seemed a good idea at the time of planning the experiments, proved difficult to implement. Heat transfer rates measured under these imprecisely defined conditions were an order of magnitude higher than those predicted from the saturated film boiling experiments on single spheres in (a) and were more characteristic of subcooled micro-bubble or disturbed film boiling, with maximum heat fluxes up to 3 MW/m^2 (Fig. 11). Flow-related measurements of pressure drops and the momentum flux leaving the array indicated large fluctuations, particularly for the lowest volume fraction of spheres. This was confirmed by video recordings with windows replacing two sides of the duct. The observations were confined to the edge of the array, where the liquid–vapour flow was so disturbed that nothing could be learned from the pictures.

In this progression of experiments, optical measurements became more difficult, and eventually impossible, as the conditions moved from idealised experiments towards those of molten fuel-coolant interactions. Perhaps the one directly useful outcome was the negative finding that expressions for interphase drag and heat transfer for simulations of large-scale FCIs cannot be reliably based on experiments on single spheres. When the industrial conditions for applications of controlled FCIs are closer to laboratory conditions (e.g. Furuya, 2002), optical observations can make a valuable contribution.

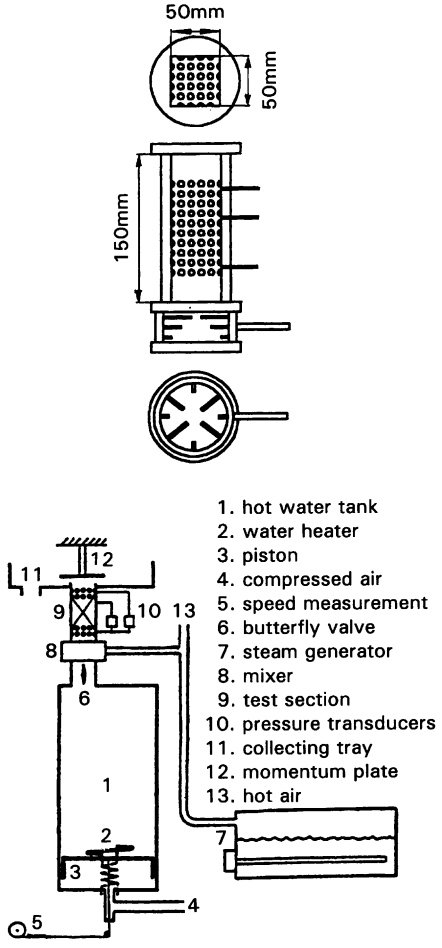

Fig. 10. Quenching experiment on an array of solid spheres.

3. Through-wall observation of boiling

3.1. Techniques

The difficulty of determining the detailed mechanisms of disturbed film boiling by viewing through the fluid is met also in saturated pool nucleate boiling on horizontal surfaces at all but the lowest heat fluxes. (Optical access normal to the surface is somewhat easier for saturated boiling on the sides of horizontal cylinders, e.g. Gorenflo et al. (1998), and for subcooled flow boiling in channels heated on only one surface, e.g. Del Valle and Kenning (1985).) Alternatively, spatio-temporal data of various sorts may be acquired by optical means through the heated wall. This always imposes special conditions of wall material, wall thickness or surface finish.

The options are

(a) Observation of the geometry of liquid–vapour interfaces through a glass, quartz or sapphire wall with a transparent thin-film heater either on the boiling surface or the rear surface, with

(i) near-normal illumination, including direct observation and interferometry;
(ii) oblique illumination, with total reflection at wall-vapour interfaces to identify dry patches.

Heaters at the boiling surface may be continuous or divided into arrays with independent control of local heat flux and electrical resistance measurement of temperature.

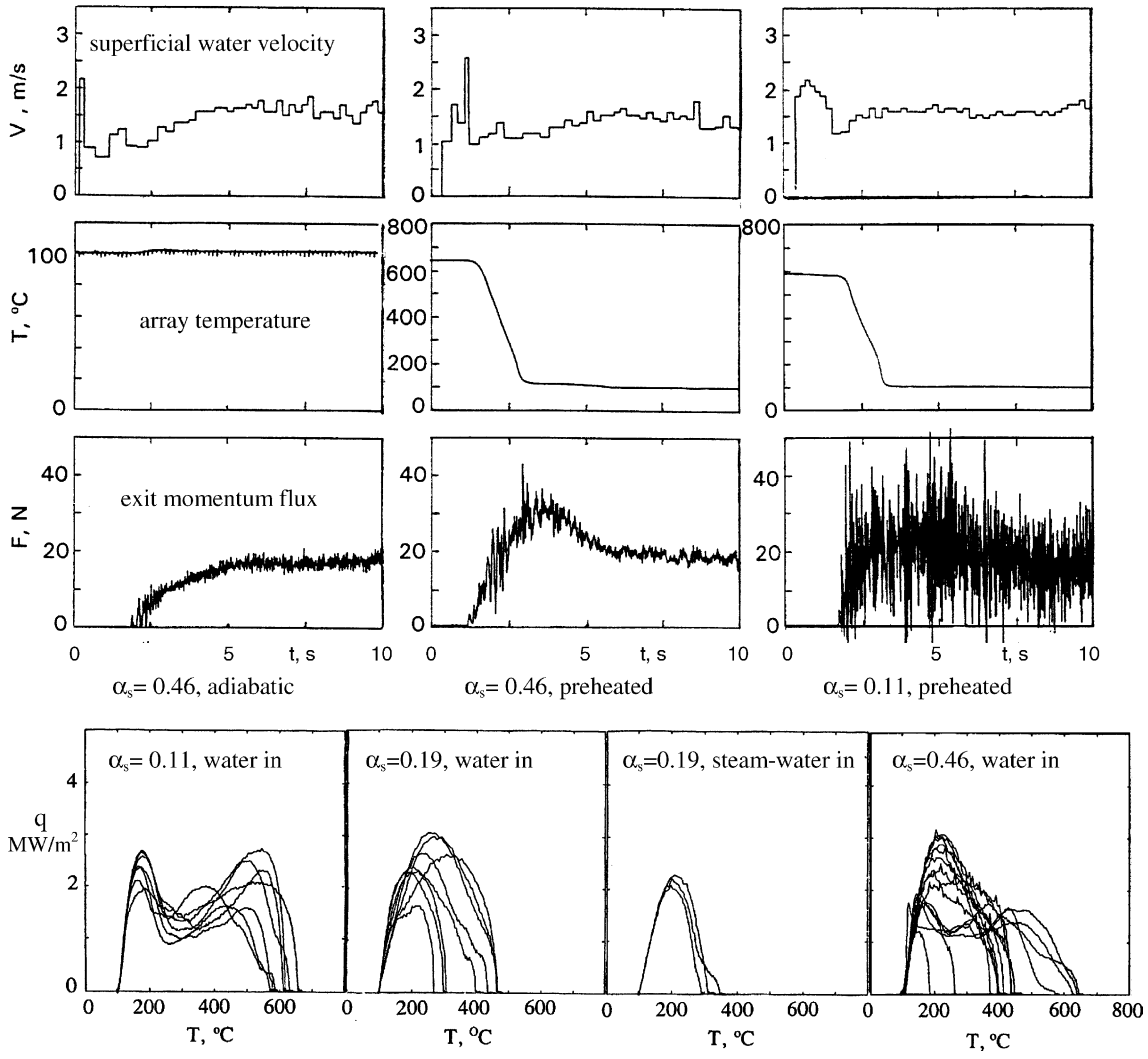

Fig. 11. Quenching experiments on arrays of spheres.

(b) Measurement of wall temperature fields with

(i) an opaque thin-film heater of low thermal impedance at the boiling surface, optical measurement of temperature at the back surface of the heater through a transparent wall;
(ii) an opaque, thin wall with optical measurement of temperature at the rear surface.

Thin-film heaters of negligible thermal capacity at the boiling surface essentially cause boiling at conditions determined by the diffusivity of the bulk wall material, except in the special case of arrays of heaters with individual feedback control (e.g. Kim et al., 2002). Glass and quartz walls have low thermal diffusivity but sapphire overlaps the diffusivity range of metals. The only option that does not constrain in some way the condition of the boiling surface is (b)(ii) but the existence of a measurable signal at the rear surface is evidence that the wall is thin enough to influence the transient flows of heat at the boiling surface.

The competing techniques for optical measurement of wall temperature are liquid crystal and I-R thermometry. Temperature-sensitive LIF does not appear to have been exploited for this particular purpose, although it may be possible to apply very thin layers of fluorescent nanoparticles. Liquid crystal must be used in layers of thickness 10 m, if unencapsulated, to 20–30 μm in the more usual and robust encapsulated form. Its low thermal conductivity makes it undesirable to pass through it the high-heat fluxes characteristic of boiling, so it is effectively limited to (b)(ii), measurements on the back of thin, electrically heated metal plates. Its low thermal diffusivity also limits its frequency response, since temperature changes have to be diffused through its thickness. It is difficult now to obtain liquid crystal with a reasonably linear relationship between temperature and hue over a range of at least 10 K at the elevated

temperatures required for the study of boiling and heating above the colour play range can cause hysteresis that limits liquid crystal thermography to relatively low heat fluxes. These inherent disadvantages compared to I-R thermometry have until recently been offset by the advantages of recording by colour video cameras in respect of speed for fully two dimensional as opposed to line measurements, in data storage in analogue mode and, apparently, in spatial resolution. However, high-speed colour cameras suffer from signal noise and their resolution measured in output pixels may be less than expected. Kono and Kenning (2001) found that a sharp boundary between two colours could be diffused over 5 pixels (Fig. 12). Very recent developments in I-R cameras mean that they now compete with video cameras in speed and resolution, with sensor arrays of 320×256 pixels at 500 Hz reducing to 128×128 pixels at 1000 Hz and digital storage of 1000 sequential fields (Theofanous et al., 2002a,b). High resolution and long-recording times are essential for the investigation of interactions between members of a large group of nucleation sites.

Next, some representative examples are given of the above techniques and the qualified insights that they provide into events at the liquid–vapour–solid boundary region in boiling. This is in no way a comprehensive account of the large and developing body of work in this region.

3.2. Interferometry and liquid crystal thermography

As discussed in more detail by Kenning (1999), optical evidence for the existence of evaporating liquid micro-layers under bubbles growing on glass with transparent surface heaters (condition (a)(i)), with a central dry spot that initially grows more slowly than the bubble, was obtained by Voutsinos and Judd (1975) for dichloromethane at low pressure and Koffman and Plesset (1983) for water and ethanol at atmospheric pressure by interferometry. Only large, low frequency bubbles were analysed but the simultaneous occurrence of quite different modes of bubble growth was noted: large bubbles at low or intermittent frequencies, small bubbles at high frequencies. Conditions under the small bubbles were not examined. As a consequence of these and similar experiments, theoretical models of bubble growth were based on micro-layer evaporation. More recent models have assumed evaporation from a much more concentrated triple contact zone near the line where the bubble apparently contacts the wall. Kenning and Yan (1996) measured the temperature fields on the back of a 28 mm $\times$ 41 mm $\times$ 0.13 mm thick electrically-heated horizontal stainless steel plate during pool boiling of water, using liquid crystal thermography at a recording rate of 200 Hz (condition (b)(ii)). They found that the mode of bubble formation on a particular plate was very sensitive to the method of cleaning, crudely differentiated by high or low contact angle. At high contact angle, there were many nucleation sites producing small bubbles at frequencies beyond the response rate of the liquid crystal. At low contact angle, sites produced much larger bubbles at low frequencies which, fortunately, were within the range of liquid crystal measurement. Even then there was a wide variation in bubble sizes and frequencies. Large bubbles were mainly formed at sites with high activation superheats. Detailed measurements of the temperature variations under a large bubble were reported (Fig. 13a) another example of biased selection for analysis because small, fast-growing bubbles were beyond the capabilities of the measuring technique. It was shown that cooling during growth was confined to the contact region under the bubble and was consistent with evaporation of a micro-layer. Subsequent numerical simulations by Golobič et al. (1996) showed that attenuation of the temperature signal, even through this thin plate, would make it difficult to distinguish between evaporation over a distributed micro-layer or at a travelling contact line. After bubble departure, there was a relatively long-waiting period while the superheat at the nucleation site recovered. There was no obvious indication of an area of influence extending beyond the maximum contact area of the bubble but recovery at one nucleation site could be interrupted by cooling at an adjacent site (Fig. 13b). Observations on the bubble side were necessary to determine whether a sudden reduction in temperature at a site was caused by local nucleation or site interaction. Because of the time-consuming nature of manual analysis, only small numbers of bubbles were examined in detail. After a break of several years, funding became

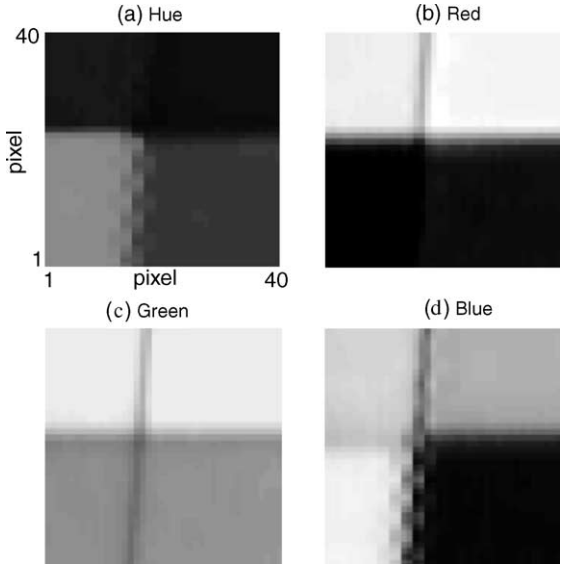

Fig. 12. 500 Hz video image of intersection of four colours on test card (Kono and Kenning, 2001).

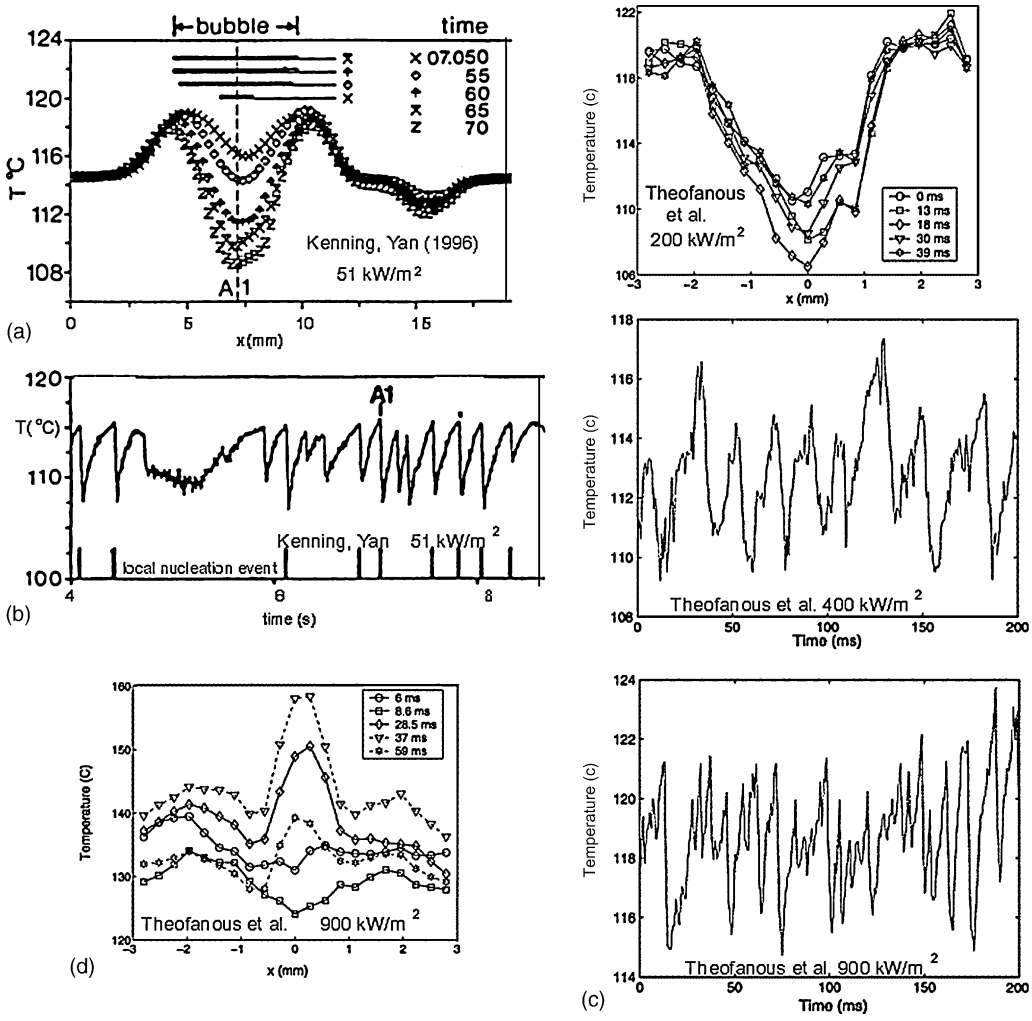

Fig. 13. Wall temperature measurements: comparison of Kenning and Yan (1996) and Theofanous et al. (2002a,b): (a, b) water on stainless steel, (c) water on titanium/glass and (d) hot spot, titanium/glass.

available to develop statistical methods of image analysis to detect nucleation events (von Hardenberg et al., 2002), and site interactions (von Hardenberg et al., 2004), based entirely on the temperature fields. Computerised analysis makes it possible to examine many examples of particular physical phenomena and to assess better their significance.

3.3. Infra-red thermography of wall temperature with fluid-phase X-radiography

Theofanous et al. (2002a) measured temperature fields for saturated water boiling on a horizontal borosilicate plate 20 mm × 40 mm × 0.13 mm thick with an opaque titanium heater of submicron thickness at the boiling surface. Path-averaged void fractions were measured at different distances above the plate by X-radiography. Temperature fields on the back of the heater were measured through the plate by I-R thermometry (condition (b)(i)) at 1000 Hz. At heat fluxes of 200 kW/m^2 and above, the temperature profiles under bubbles and the temperature variations at a nucleation site are still remarkably similar to those measured by Kenning and Yan at lower heat fluxes, except that the recovery times between bubbles are shorter at the higher fluxes and there are larger variations in the peak temperatures (Fig. 13c). (As it is impossible to obtain a direct view of the bubbles, it would be necessary to examine the development of the temperature patterns in order to know for sure whether all the temperature drops are due to local nucleation or interactions with other sites.) This behaviour persists to much higher heat fluxes, well beyond the range of measurement by liquid crystal thermography. As the critical heat flux is approached, transient hot spots appear, initially at the centres of a few of the cooled spots (Fig. 13d). Irreversible heating and spreading of one of these dry spots is identified with burnout by failure of the heater at around 400 °C. The changes in temperature patterns with increasing heat flux are

shown in Fig. 14a. Note the persistence of patterns associated with the nucleation of individual bubbles over most of the surface right up to CHF. This behaviour is similar, up to about 80% of CHF, with observations (without temperature field measurement) by Chung and No (2003) of bubble growth and dry spot development by simultaneous application of normal observation (condition (a)(i)) and the total reflection technique (condition (a)(ii)) for R-113 boiling on a horizontal sapphire plate 10 mm thick with a transparent ITO heater on its rear surface (Fig. 14b). Dry spots below the centres of bubbles occur at lower heat fluxes in R-113. Beyond 80% CHF, multiple coalescences cause large numbers of dry patches separated by wriggling networks of liquid, as previously observed with R113 on sapphire by Nishio et al. (1998).

3.4. Mechanisms of nucleate boiling and critical heat flux

The discussion by Theofanous et al. (2002a,b) of their very detailed observations, obtained under highly controlled conditions, provides a classic example of how optical observations can prompt re-examination of established ideas about nucleate boiling, both at low and near-critical heat fluxes:

(1) The nature of nucleation sites, surface ageing and surface wetting quantified by contact angle measurements.

Nucleation occurred in these experiments at superheats corresponding to site diameters of a few microns, even though the thickness of the surface heater was a fraction of a micron. The characterisation of the vapour-deposited titanium heater by SEM at magnifications of ~50,000 showed that ageing the surface by

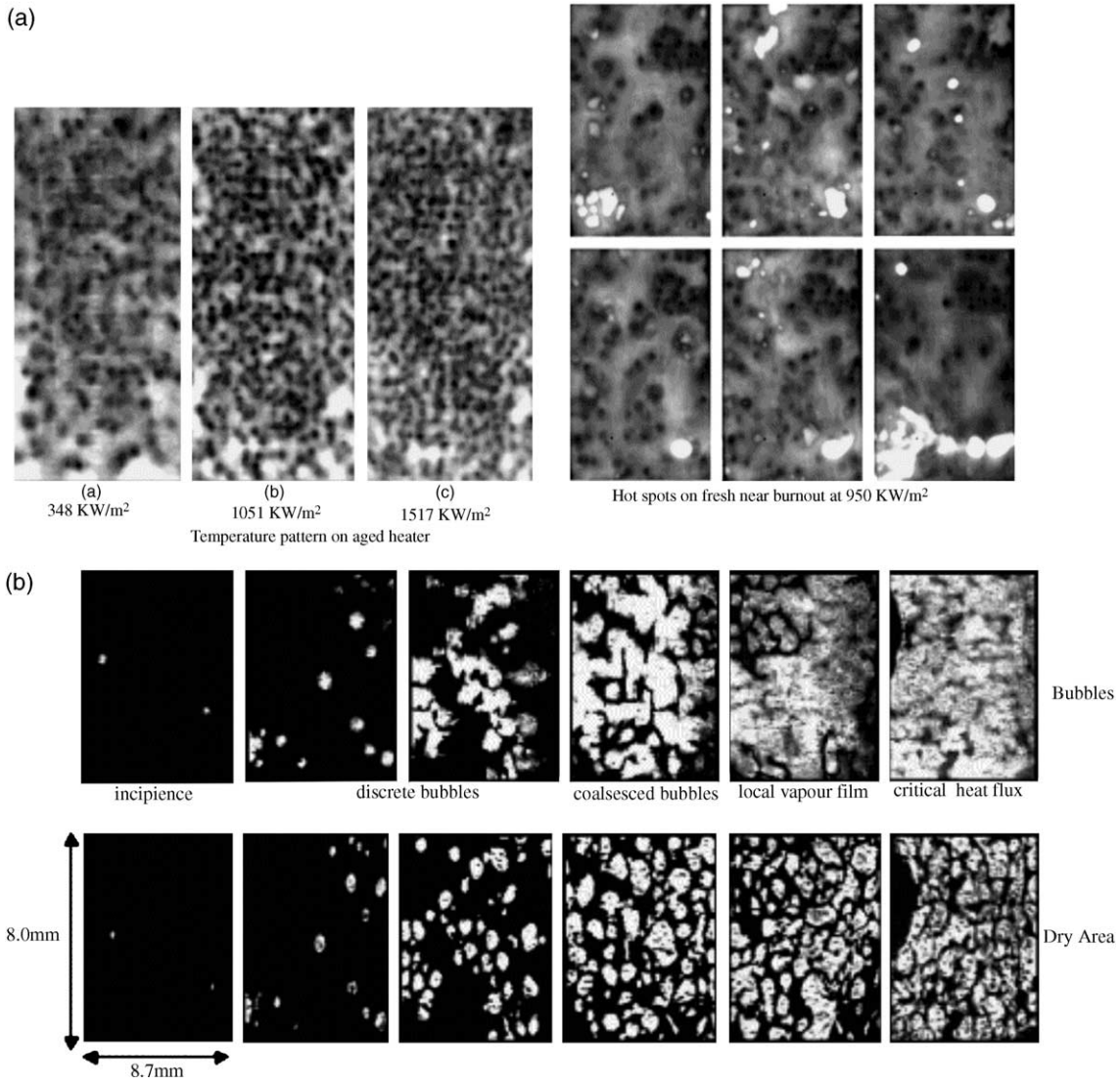

Fig. 14. (a). Temperature fields for water on titanium/glass (Theofanous et al., 2002a,b) and (b) bubble images and dry areas for R113 on sapphire, increasing heat flux (Chung and No, 2003).

repeated pulse heating through a phase transformation at 380 °C created a large number of oxide islands with dimensions below 0.5 μm. Ageing caused a significant increase in the density of nucleation sites in the I-R images, with a corresponding increase in the critical heat flux, but had no effect on the measured contact angle, which remained in the range 60–75°. The authors suggest that nucleation at low superheats on surfaces of this smoothness calls into question the concept of nucleation sites as cavities. Even at the highest CHF, the nucleation site density was only 0.6/mm^2. At the magnification required to detect micron-sized cavities, the area in a SEM image might typically be less than 50 μm × 50 μm so it is difficult to be sure of detecting such low densities of larger cavities on the glass substrate. It will be interesting to hear from the authors whether the nucleation sites were indeed fixed in position and whether they were able to detect optically any common geometrical features at the sites.

For surfaces of high textural uniformity of this sort, as for those produced in a very different way by Luke et al. (2002) by sandblasting and emery grinding of metal surfaces, there is an unresolved question of what counts as a nucleation site and how to define nucleation site density. Theofanous et al. define it as the number of bubbles captured per frame, averaged over 1000 frames, which is appropriate for stable sites producing bubbles with negligible waiting times. Gorenflo et al. (1998) discuss the significant difference between the number of sites according to a similar definition and the number seen to produce at least one bubble over a long period during boiling of refrigerants on horizontal cylinders. Kenning et al. (2001) found examples of exchange of activity between closely-situated sites. Boiling at high subcooling or saturated boiling on thin, well-wetted plates may have waiting times between bubbles that exceed growth times, so that some sites appear in only a fraction of the samples. It is noted in passing that the secondary nucleation hypothesis of Mesler (1992), that free nuclei dissociated from surface sites are produced by the interfacial breaking of larger bubbles or droplet impingement, has gone out of vogue, although its significance has never been fully proved or disproved.

(2) Theofanous et al. (2002a,b) proved by experimental subdivision of their heater that it was large enough to be effectively infinite, so that its dimensions, and those of the container, did not impose an external length scale. Their X-ray images revealed chaotic flow patterns in the liquid–vapour space with high averaged void fractions close to the surface but no evidence of the structures or length scales that would be expected either from the counterflow hydrodynamic instability model of critical heat flux or current models for high-flux boiling based on large numbers of small vapour columns penetrating a macrolayer under a large hovering vapour mass, developed from Gaertner's (1965) reports of observations with a restricted side view of what may be unrepresentative events at the edge of the region. They argue for "scale separation" between events in the fluid region and the controlling events on the heated surface, where they suggest that the crucial length scale is the distance between active nucleation sites. They produce evidence that disturbances from active sites promote rewetting of developing dry patches. The fluid region must still have a role as the source of liquid to replenish the thin liquid layer on the wall, in which nucleate boiling persists up to burnout, but it is suggested that the details of its motion, including weak convection, may not influence the instability of dry patches that leads to burnout.

(3) The observations were made for boiling on a thin glass substrate so that transient conduction, which plays an essential part in controlling the irreversible local heating at a dry spot that triggers critical heat flux, may be very different from conditions on substrates with thermal diffusivities typical of metals. The paper refers to similar experiments on a sapphire substrate so this desirable information may be available by the time this review appears. In flow boiling of water at high subcooling and heat fluxes up to 7 MW/m^2, burnout is accompanied by tiny pinholes melted through a thin stainless steel strip (Del Valle, 1980).

The authors of these remarkable optical observations have been careful to define their range of validity for "scale separation". Even then, there is some evidence of rather different behaviour at the critical heat flux for a different fluid/surface combination. More work is required to determine whether the surface employed in this work has special nucleation characteristics, in which case the failure of conventional CHF models for these conditions may not necessarily mean that they are invalid in all situations. In other applications, such as the forced convective boiling on spheres described in Section 2, the external conditions may impose additional physical mechanisms that interact with the mechanisms at the surface.

4. Concluding remarks

This paper has considered only a small fraction of the optical methods relevant to the investigation of boiling heat transfer. Optical methods of tracking and sizing swarms of bubbles, or of measuring the local flow fields in the liquid phase by LDA or PIV, e.g. combined with liquid crystal temperature tracers (Pakleza et al., 2002) have not been discussed. They present considerable difficulty because of the fully three-dimensional nature of the fields that develop even in systems with nominal axial symmetry. The even more challenging problem of simultaneous measurement of flow, temperature and

concentration fields during boiling of mixtures has yet to be addressed by researchers.

The message of this paper has been that the insights provided by optical methods are invaluable but there are risks of misapplication because

(i) the implementation of any optical technique constrains the design of the experiment;
(ii) the range of conditions that can be studied is limited by the demands of the technique and the time required to perform and process difficult experiments.

Readers should always go back to the original papers to check the limitations specified by authors and proceed with caution outside those limits.

It is clear that insights are still needed when such fundamental questions as the role of the triple interface in bubble growth and in the mechanisms of high-flux boiling are still open to debate. Understanding and controlling the influences of surface micro-geometry and physico-chemistry in laboratory experiments and then applying the findings to industrial systems where such control is not possible still cause major difficulties. Efficient use of hard-won experimental data within their range of validity requires careful planning of their role in the improvement and validation of numerical simulations that can now be performed with ever-increasing sophistication.

References

Aziz, S., 1986. Forced convection film boiling on spheres. In: D.Phil. Thesis. Dept. Eng. Science, University of Oxford.

Aziz, S., Hewiit, G.F., Kenning, D.B.R., 1986. Heat transfer regimes in forced-convection film boiling on spheres. In: Proceedings of 8th International Heat Transfer Conference, vol. 5. San Francisco, pp. 2149–2154.

Chen, S., Kenning, D.B.R., 1996. Drag on arrays of solid spheres in steam-water flows. In: Proceedings of 2nd European Thermal-Sciences and 14th UIT National Heat Transfer Conference, vol. 3. Rome, pp. 1581–1587.

Chung, H.J., No, H.C., 2003. Simultaneous visualization of dry spots and bubbles for pool boiling of R-113 on a horizontal heater. Int. J. Heat Mass Transfer 46, 2239–2251.

Cooper, M.G., 1983. The mirage in boiling. Int. J. Heat Mass Transfer 26, 1088–1090.

Cooper, M.G., Chandratilleke, T.T., 1981. Growth of diffusion-controlled vapour bubbles at a wall in a known temperature gradient. Int. J. Heat Mass Transfer 24, 1475–1492.

Correll, S., 1989. Flow film boiling on levitated molten drops and vapour explosion triggering. D.Phil. Thesis, Dept. Eng. Science. University of Oxford.

Correll, S., Kenning, D.B.R., 1992. Subcooled flow boiling on molten drops at 1100 °C. In: Proceedings of Engineering Foundation Conference on Pool and Flow Boiling, Santa Barbara, pp. 303–308.

Del Valle, M.V.H., 1980. Flow boiling near the critical heat flux. D.Phil. Thesis, Dept. Eng. Science. University of Oxford.

Del Valle, M.V.H., Kenning, D.B.R., 1985. Subcooled flow boiling at high heat flux. Int. J. Heat Mass Transfer 28, 1907–1920.

Furuya, M., 2002. Development of novel rapid cooling and atomisation process making the best use of vapor explosion phenomena. In: Proceedings of 12th International Heat Transfer Conference, vol. 4. Grenoble, pp. 705–710.

Gaertner, R.F., 1965. Photographic study of nucleate pool boiling on a horizontal surface. J. Heat Transfer 87, 17–29.

Golobič, I., Pavlovič, E., Strgar, S., Kenning, D.B.R., Yan, Y., 1996. Wall temperature variations during bubble growth on a thin plate: computation and experiment. In: Proceedings of Eurotherm Seminar No. 48 Pool Boiling, vol. 2. Paderborn, pp. 25–32.

Gorenflo, D., Luke, A., Danger, E., 1998. Interactions between heat transfer and bubble formation in nucleate boiling. In: Proceedings of 11th International Heat Transfer Conference, vol. 1. Kyongju, pp. 149–174.

Katto, Y., 1992. Critical heat flux in pool boiling. In: Proceedings of Engineering Foundation Conference on Pool and Flow Boiling. Santa Barbara, pp. 151–164.

Kenning, D.B.R., Yan, Y., 1996. Pool boiling heat transfer on a thin plate: features revealed by liquid crystal thermography. Int. J. Heat Mass Transfer 39, 3117–3137.

Kenning, D.B.R., 1999. What do we really know about nucleate boiling? In: IMechE Conference Transactions of 6th UK Conference on Heat Transfer. Edinburgh, pp. 143–167.

Kenning, D.B.R., 2001. Experimental methods: looking closely at bubble nucleation. Multiphase Sci. Technol. 13, 1–33.

Kenning, D.B.R., Kono, T., Wienecke, M., 2001. Investigation of boiling heat transfer by liquid crystal thermography. Exp. Therm. Fluid Sci. 25, 219–229.

Kim, J., Benton, J.F., Wisniewski, D., 2002. Pool boiling heat transfer on small heaters: effect of gravity and subcooling. Int. J. Heat Mass Transfer 45, 3919–3932.

Koffman, L.D., Plesset, M.S., 1983. Experimental observations of the microlayer in vapor bubble growth on a heated solid. Trans. ASME J. Heat Transfer 105, 625–632.

Kono, T., Kenning, D.B.R., 2001. Resolution of a high-speed video camera used for liquid crystal thermography of wall temperatures in nucleate boiling. In: 7th UK National Conference on Heat Transfer. Nottingham September 11–12, 2001.

Luke, A., Danger, E., Gorenflo, D., 2002. Size distribution of actual and potential nucleation sites in pool boiling. In: Proceedings of 12th International Heat Transfer Conference, vol. 3. Grenoble, pp. 383–388.

Mayinger, F., 1995. Advanced optical methods. In: Proceedings of International Conference on Convective Flow Boiling. Banff, pp. 15–28.

Mesler, R.L., 1992. Improving nucleate boiling using secondary nucleation. In: Proceedings of Engineering Foundation Conference on Pool and Flow Boiling. Santa Barbara, pp. 43–48.

Nishio, S., Gotoh, N., Nagai, N., 1998. Observation of boiling structures in high heat-flux boiling. Int. J. Heat Mass Transfer 41, 3191–3201.

Pakleza, J., Duluc, M.-C., Kowalewski, T., 2002. Experimental investigation of vapor bubble growth. In: Proceedings of 12th International Heat Transfer Conference, vol. 3. Grenoble, pp. 479–484.

Stevens, J.W., Witte, L.C., 1971. Transient and transition film boiling from a sphere. Int. J. Heat Mass Transfer 14, 443–444.

Theofanous, T.G., Tu, J.P., Dinh, A.T., Dinh, T.N., 2002a. The boiling crisis phenomenon—Part I: nucleation and nucleate boiling heat transfer. Exp. Therm. Fluid Sci. 26, 755–792.

Theofanous, T.G., Dinh, T.N., Tu, J.P., Dinh, A.T., 2002b. The boiling crisis phenomenon—Part II: dryout dynamics and burnout. Exp. Therm. Fluid Sci. 26, 793–810.

von Hardenberg, J., Kono, T., Kenning, D.B.R., McSharry, P.E., Smith, L.A., 2002. Identification of boiling nucleation sites by non-orthogonal empirical functions (NEF) analysis of thermographic

data. In: Proceedings of 12th International Heat Transfer Conference, vol. 3. Grenoble, pp. 377–382.

von Hardenberg, J., Kenning, D.B.R., Xing, H., Smith, L.A., 2004. Identification of nucleation site interactions. Int. J. Heat Fluid Flow, this issue. doi:10.1016/j.ijheatfluidflow.2003.11.015.

Voutsinos, C.M., Judd, R.L., 1975. Laser interferometric investigation of the microlayer evaporation phenomenon. Trans. ASME J. Heat Transfer 97, 88–92.

Zvirin, Y., Hewitt, G.F., Kenning, D.B.R., 1990. Boiling on free-falling spheres: drag and heat transfer coefficients. Exp. Heat Transfer 3, 185–214.